EARTHQUAKE RESISTANT DESIGN OF EARTH FILL DAM BASED ON LABORATORY SOIL TESTS

K. Uchida(I) and T. Hasegawa(II)

SYNOPSIS

This paper examines the fundamental aspects for earthquake resistant design of earth fill dams based on laboratory soil tests. By cyclic triaxial test of a soil subjected to initial shear stress, the cyclic deformation and strength characteristics are quantitatively evaluated. Then, the failure mechanism of fill dams during earthquakes is clarified by the dynamic failure test of a fill dam model using shaking table apparatus. Finally, strain potential of the dam model analysed by FEM is comparable with the experimental results to verify the applicability of this procedure to practical problems.

INTRODUCTION

It is a fundamental subject for developing consistent earthquake resistant design of earth fill dams to clarify the failure mechanism and the factors affecting on the failure during earthquakes. The previous seismic damages for earth fill dams are summarized in cracking on the crest, partial slide or heave at the upper portion of a slope, and subsequent slope failure or settlement of the crest leading to the catastrophic failure of the dams. These damages agree with the experimental results of the dynamic failure tests of shaking table dam models (Refs.1 and 2). These facts suggest that permanent deformation of soil under a sloping surface is one of the most important factors affecting on the failure of earth fill dams during earthquakes. Since the soil under a sloping surface is subjected to initial shear stress prior to seismic loading, the seismic behavior of this soil may be affected by the presence of initial shear stress, and so recently these effects have been investigated extensively, involving offshore problems.

This paper examines the dynamic failure mechanism and cyclic deformation and strength characteristics of soil under a sloping surface by cyclic triaxial test and shaking table model test. The purposes of this paper are as follows : (1) to clarify the failure mechanism and the major factors affecting on the failure during earthquakes ; (2) to define the dynamic strength of soil subjected to initial shear stress ; (3) to quantitatively determine permanent axial strain and residual pore pressure based on the cyclic triaxial test results ; (4) to analyse strain potential of the dam model using the FEM program incoporated these relations to verify the applicability of this procedure to practical problems concerned with earthquake resistant design.

CYCLIC TRIAXIAL TEST OF A SOIL SUBJECTED TO INITIAL SHEAR STRESS

Experimental Program

The testing material used in this study is an actual fill dam material, physical properties of which are listed in Table 1. Specimens 5*cm* in diameter by 10*cm* in height are prepared by pouring the saturated soil into a mold filled with deaired water in advance and by tapping around the mold with a small wooden hammer to adjust a desired initial void ratio between 0.55 and 0.70. In order to ensure full saturation, pore pressure coefficient B is

(I) Lecturer of Agricultural Engineering, Kyoto University, Kyoto, JAPAN
(II) Professor of Agricultural Engineering, Kyoto University, Kyoto, JAPAN

Table 1. Physical properties of soil

Specific Gravity	G_s	2.649
Grading	D_{10}	0.0060 mm
	D_{50}	0.48 mm
	U_c	116.7
	F.C.	7.71
Limit Density (in saturated condition)	e_{max}	0.814
	e_{min}	0.535

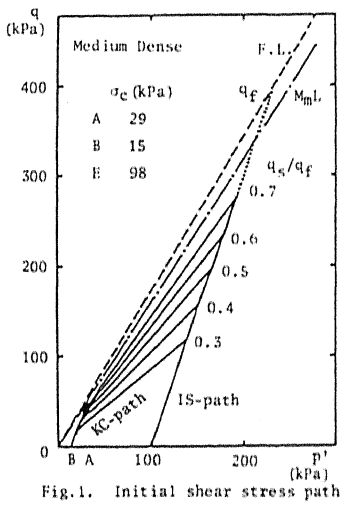

Fig.1. Initial shear stress path.

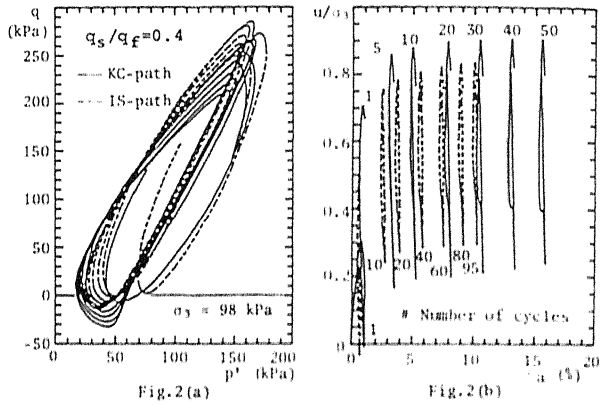

Fig.2(a) Fig.2(b)

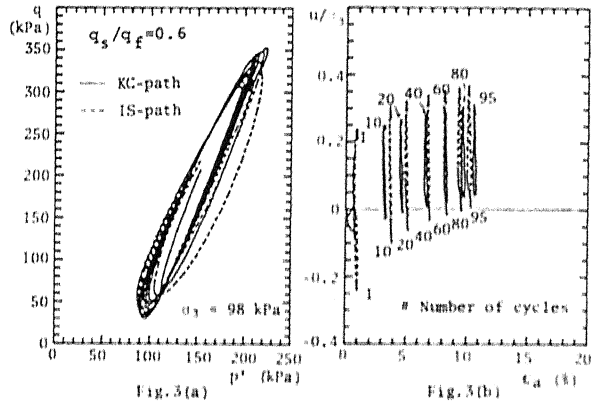

Fig.3(a) Fig.3(b)

Figs.2,3. Cyclic behavior of soil subjected to initial shear stress (Fig.2: q_s/q_f=0.4, Fig.3: q_s/q_f=0.6, (a) cyclic stress path, (b) axial strain vs pore pressure).

confirmed to be greater than 0.96 before isotropic consolidation and back pressure of 98*kPa* (1.0*kgf/cm*^{2}) is applied. The testing system is constituted of a servo controlled cyclic triaxial apparatus and a micro computer equipped with A/D and D/A converters. The initial shear loading paths controlled by the computer are, as shown in Fig.1, the isotropic consolidation and drained shear path (which will be abbreviated *IS-path*), the anisotropic consolidation path (abbreviated *KC-path*), and the K_0 consolidation path as a special case of *KC-path*. Initial shear stress levels are varied in the wide range of q_s/q_f 0.0 to 0.7 ; q_s is initial deviator stress and q_f deviator stress at static failure. The sinusoidal cyclic axial load of 1/*Hz* frequency is applied under undrained condition with confining stress σ_3 held constant (σ_3 98*kPa* for *IS-path* ; σ_3=49 and 98*kPa* for *KC-path*).

Test Results

Figs.2 and 3 show the typical results of cyclic triaxial test with initial shear loading using *IS-path* and *KC-path* ; in which, (a) the cyclic stress path described in the relation between effective mean principal stress p' and deviator stress q, (b) the relation between axial strain ε_a and the ratio of pore pressure u to confining stress σ_3, q_s/q_f=0.4 and 0.6, σ_3=98*kPa*, and almost the same void ratio before cyclic loading. The following characteristics for cyclic behavior of soil subjected to initial shear stress are recognized commonly for the two kinds of path : (1) permanent axial strain

increases with number of cycles ; (2) on applying the same cyclic stress, residual pore pressure decreases with increasing initial shear stress level ; (3) axial strain amplitude develops to the maximum limit within 1%. Refs.3-5 pointed out similar characteristics. On comparing these figures, it is found that the specimens exhibit the similar cyclic behavior for different initial stress paths and for different confining stresses, if there are no significant differeces of the degree of shear stress reversal (Ref.6) and of stress and strain state before cyclic loading, and if normalized by confining stress σ_3.

Dynamic Strength of Soil Subjected to Initial Shear Stress

Judging from the characteristics of the cyclic behavior mentioned above, permanent strain seems to be a key to define the dynamic strength of that soil. Fig.4 shows the typical results described in the relation between number of cycles N and permanent axial strain ε_a during cyclic loading. This N-ε_a curve tends to be convex upward at the beginning and to gradually approach to a straight line. A shifting point from a curve to a straight line means a point reaching constant increment of permanent axial strain $\Delta\varepsilon_a$ or constant strain velocity. When introducing the concept of creep failure that materials may fail in time on reaching constant strain velocity, this point possibly means a start point of dynamic failure. A quadratic curve approximation is applied to the N-$\Delta\varepsilon_a$ data so that the start point of dynamic failure is determined by the point with the variation of $\Delta\varepsilon_a$ in each cycle reaching 10^{-3} %. Moreover, it is examined if there is a correlation between $\Delta\varepsilon_a$ at the start point of dynamic failure and a specified permanent axial strain ε_a, since the criterion defined by permanent strain is easier to apply than the one by increment of permanent strain. In Fig.5, the abscissa is the $\Delta\varepsilon_a$ value with the variation of $\Delta\varepsilon_a$ in each cycle reaching 10^{-3} % and the ordinate is the $\Delta\varepsilon_a$ value of permanent axial strain ε_a reaching the specified value (examined from 5 to 12%). The solid line indicates the line determined by the method of least squares and the dotted line indicates the line of unit gradient through the origin. It is seen that the two lines in each figure do not agree for ε_a=5 to 8% but they nearly agree for ε_a above 9% or 10%, and that the mutual position of the two lines does not change with increasing ε_a above 10% because the increment has reached a constant value. This result has the significances that the dynamic strength can be defined by a specified permanent axial strain, 9% or 10% for this testing soil, and that the

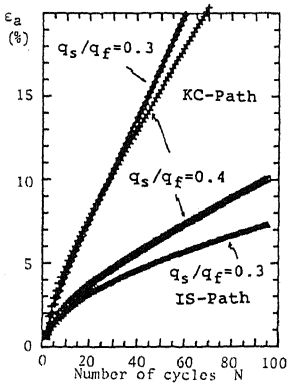

Fig.4. Number of cycles N vs permanent axial strain ε_a.

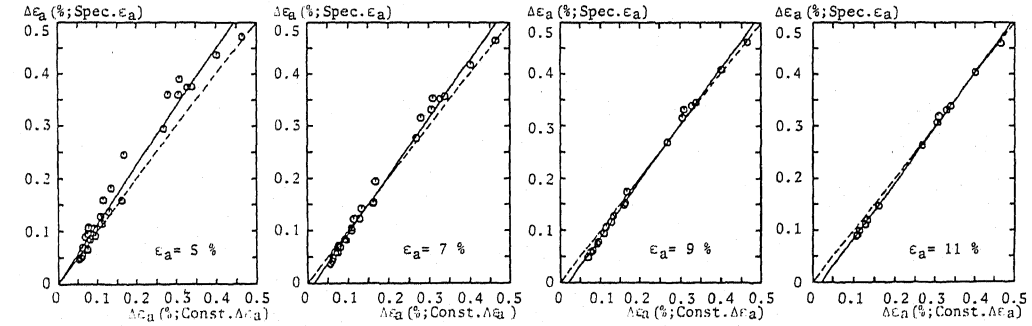

Fig.5. Correlation between increments of permanent axial strain $\Delta\varepsilon_a$ defined by $\Delta\varepsilon_a$ reaching constant and by a specified permanent axial strain ε_a.

basis for dynamic failure criterion is specified by corresponding to the start point of dynamic failure defined by constant increment of permanent axial strain. There were several dynamic failure criteria defined by axial strain of 10% (e.g. Refs.7-9), none of which specified any basis.

Quantitative Determination of Permanent Axial Strain

Quantitative determination is examined for permanent axial strain and pore pressure build-up which characterize cyclic triaxial behavior of soil subjected to initial shear stress so that these test results can be applied to practical problems concerned with earthquake resistant design. The procedure proposed by Ref.5 is used for this purpose because all the following parameters related to developing permanent axial strain can be considered : void ratio before cyclic loading (e_s), the ratio of the mean value of cyclic effective mean principal stresses in each cycle p_m to confining stress σ_3 (p_m/σ_3), the ratio of the mean value of cyclic deviator stresses in each cycle q_m to p_m (q_m/p_m), the ratio of cyclic stress amplitude q_a to p_m (q_a/p_m), and number of cycles (N). Figs. 6, 7 and 8 indicate the relations among permanent axial strain ε_a and the above five parameters, where the variations of three parameters among the four are restricted in small ranges. As shown in these figures, the contour lines of strain can be generally expressed in $y=a+b\log N$, and the gradients of these lines are independent of the values of the restricted parameters and are constant : $b_e=-0.15$ for e_s ; $b_{p_m}=-1.20$ for p_m/σ_3 ; $b_{q_a}=-0.70$ for q_a/p_m. Then, the data shown in these figures are transformed to one set of reference values using equivalent number of cycles N_e as follows :

$$N_e=N\cdot 10^{((e_s)_{ref}-e_s)/b_e}=C_e\cdot N \qquad (1)$$

$$N_e=N\cdot 10^{((p_m/\sigma_3)_{ref}-p_m/\sigma_3)/b_{p_m}}=C_{p_m}\cdot N \qquad (2)$$

$$N_e=N\cdot 10^{((q_a/p_m)_{ref}-q_a/p_m)/b_{q_a}}=C_{q_a}\cdot N \qquad (3)$$

Fig.9 gives the relation between permanent axial strain ε_a and equivalent number of cycles N_e ($=C_e\cdot C_{p_m}\cdot C_{q_a}\cdot N$) for several constant values of q_m/p_m with the data transformed by the above procedure to the set of reference values $e_s=0.55$, $p_m/\sigma_3=1.0$, and $q_a/p_m=1.0$. It is shown that a linear relation exists between the logarithms of N_e and of permanent axial strain ε_a.

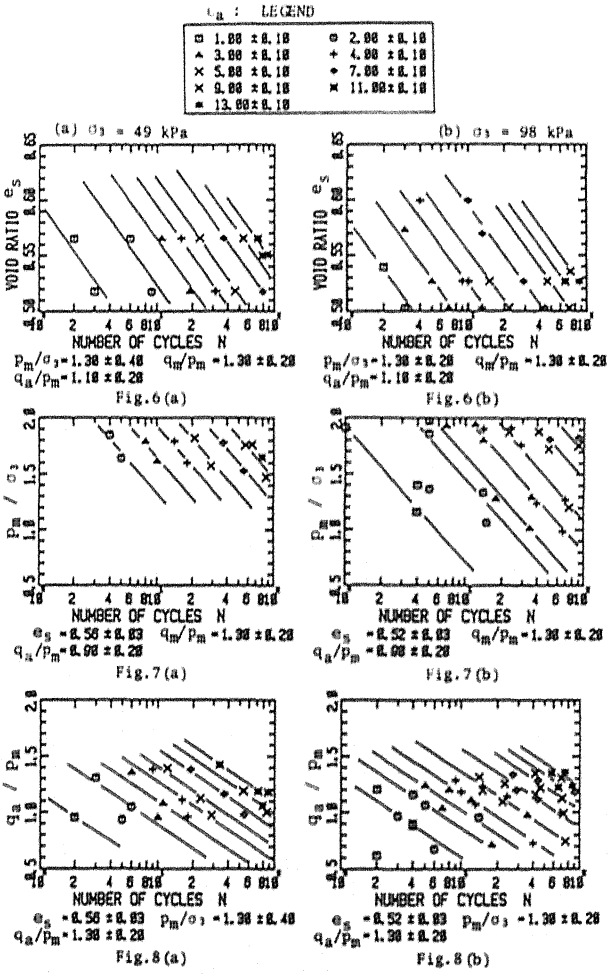

Fig.6.7.8. Contours of permanent axial strain .
(Fig.6. for e_s, Fig.7. for p_m/σ_3, Fig.8. for q_a/p_m)

$$\varepsilon_a = f(q_m/p_m) \cdot (N_e)^A \qquad (4)$$

in which A is the gradient of parallel straight lines, from Fig.9, A=0.53. Fig.10 shows permanent axial strain at N_e=1, or $f(q_m/p_m)$ in Eq.(4), varying with q_m/p_m. It is found from this figure that permanent axial strain ε_a at N_e=1 increases with increasing q_m/p_m in lower initial shear stress levels, but decreases with increasing q_m/p_m above 1.0 because negative pore pressure develops. Consequently, permanent axial strain can be quantitatively determined by the above procedure.

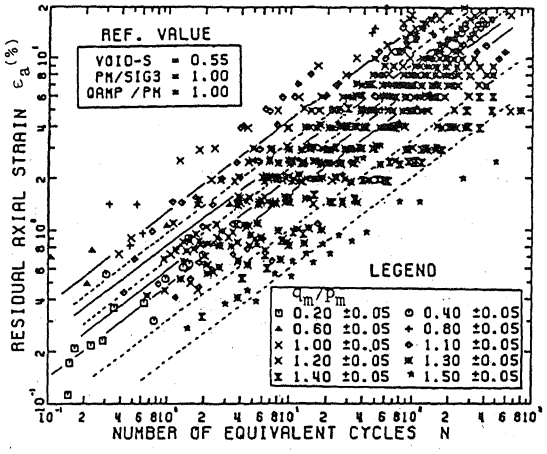

Fig.9. Average contours of permanent axial strain for different values of q_m/p_m.

Quantitative Determination of Residual Pore Pressure

From the figures for the relation between permanent axial strain ε_a and the pore pressure ratio $\bar{U}(=u/\sigma_3)$, it is seen that the effects of applying initial shear stress on pore pressure build-up during cyclic loading are the decrease of residual pore pressure level with increasing inital shear stress level and the occurrence of negative pore pressure in higher initial shear stress levels, and that pore pressure except at first cycle increases monotonously. So, the quantitative determination of the pore pressure ratio at first cycle $\bar{U}_{N=1}$ and at the subsequent cycle $\bar{U}-\bar{U}_{N=1}$ are examined separately with the following parameters ; void ratio before cyclic loading (e_s), initial shear stress level (q_s/q_f), and ratio of cyclic stress amplitude q_a to confining stress σ_3 (q_a/σ_3). Fig.11 shows the result of multiple regression analysis among the parameters and the pore pressure ratio at first cycle $\bar{U}_{N=1}$. It is seen that $\bar{U}_{N=1}$ is independent of the magnitude of q_a/σ_3 and can be expressed using e_s and q_s/q_f as follows :

$$\bar{U}_{N=1} = 2.44 \cdot e_s - 1.0 \cdot (q_s/q_f) - 0.78 \qquad (5)$$

This result means that pore pressure at first cycle is controlled by the soil fabric constructed in initial shear process. The application of Eq.(5) is restricted in q_s/q_f>0.2. The magnitude of $\bar{U}_{N=1}$ for q_s/q_f<0.2 may be less than the one predicted by Eq.(5) and may depend on q_a/σ_3. But there are no sufficient data for q_s/q_f<0.2 to be examined further. Then, a hyperbolic relation is applied between pore pressure ratio at after

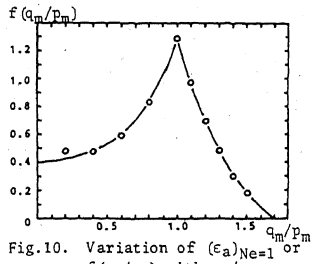

Fig.10. Variation of $(\varepsilon_a)_{Ne=1}$ or $f(q_m/p_m)$ with q_m/p_m.

LEGEND (for Figs.11,13,14.)

e_s \ q_a/σ_3	1.00	1.25	1.50	1.75	2.00	2.25	2.50	2.75
0.48	○	⊕	◎	⊙	◐	◑	⊖	⊜
0.50	△	▲	▲	▲	▲	▲	▲	▲
0.52	□	⊞	⊡	⊡	◧	◨	▣	▣
0.54	◇	◆	◆	◆	◆	◆	◆	◆
0.56	◇	◆	◆	◆	◆	◆	◆	◆
0.58	▽	▼	▽	▼	▼	▼	▼	▽

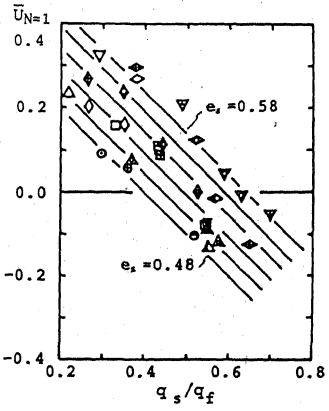

Fig.11. Multiple regression analysis among $U_{N=1}$, e_S, q_S/q_f and q_a/σ_3.

second cycle $\overline{U}-\overline{U}_{N=1}$ and permanent axial strain ε_a :

$$\overline{U}-\overline{U}_{N=1}=\varepsilon_a/(\alpha+\beta\cdot\varepsilon_a) \qquad (6)$$

Fig.12 shows a close agreement between the hyperbolic relation Eq.(6) and the test data in a wide range from the beginning of cyclic loading to close failure. The reciprocals of the coefficients α and β mean the initial tangent modulus and the asymptotic value respectively. The results of the multiple regression analysis among the coefficients α, β and the parameters e_s, q_s/q_f, q_a/σ_3 are shown in Figs.13 and 14 respectively. It is shown in these figures that the coefficients α and β depend on only q_s/q_f, independently of e_s and q_a/σ_3 and that the relations between α, β and q_s/q_f can be quantitatively determined by the method of least squares as follows :

$$\alpha=0.25\cdot(4000)^{q_s/q_f} \qquad (7)$$
$$\beta=1.1\cdot(10)^{q_s/q_f} \qquad (8)$$

Eq.(8) is essentially the same as the equation shown in Ref.10 as shown in Fig.14 :

$$(\Delta U_r)_{term}/\sigma_{3_c}=1-(K_c-1)\cdot(1-\sin\varphi)/(2\sin\varphi)=1-(q_s/q_f) \qquad (9)$$

It is concluded that residual pore pressure can be quantitatively determined by Eqs.(5) to (8) using the data e_s, q_s/q_f and σ_3.

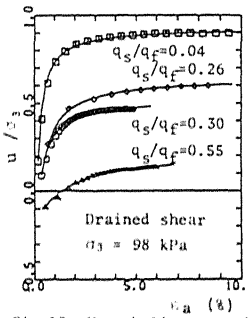

Fig.12. Hyperbolic approximation of ε_a — u/σ_3

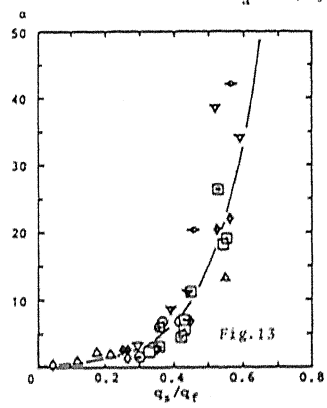

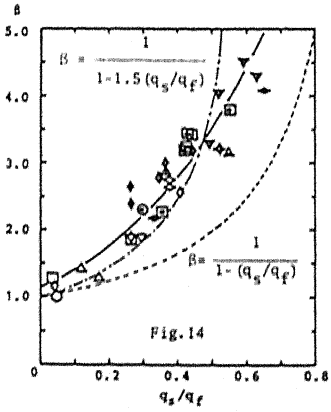

Fig.13,14. Multiple regression Analysis among coefficients α, β and parameters e_s, q_s/q_f, q_a/σ_3.

SHAKING TABLE MODEL TEST

Dynamic failure test of a fill dam model was performed by the shaking table apparatus (Ref.2) in order to measure acceleration and pore pressure developing in a dam model during cyclic loading and to verify the failure mechanism of it. The model (height H=45*cm*, base length 230*cm* and width 60*cm*) had the scale of 1/100 to the prototype dam and was made of the same fill material as used in the cyclic triaxial test. The dry density of the material compacted by a vibrating tamper, 16.6*kN/m*^{3} (1.69 *gf/cm*^{3}), was about the same as that of the prototype dam and the degree of saturation under a phreatic surface was 90 to 100% which was obtained by replacement CO_2 with water. 8 accelerometers and 5 pore pressure transducers were mainly instrumented in the upstream portion of the model. The measured data recorded by a data recorder were analysed by the micro-computer. The test was performed with water level held 0.78H (35*cm*) to prevent overtopping. And sine wave acceleration was used of 130 *gals* (for 30 *sec*), 200 *gals* (for 60 *sec*) and 300 *gals* (for 70 *sec*) amplitude and of 15*Hz* frequency, which is estimated to be a resonance frequency at higher amplitude from the result of the 25 *gals* sine wave sweep test (the first resonance frequency 25*Hz*). During the 200 *gals* test, water floating and heave were

observed at the downstream slope. After the 300 *gals* test, the partial slope failure occurred near the exit portion of the phreatic surface at the downstream slope, and settlement of the crest was about 0.1H (4*cm*) but no overtopping occurred. Fig.15 shows transverse configurations and displacements of the accelerometers after the test. From this figure, the slides are recognized to occur, consisted of the large one at the middle-lower portion of the downstream slope and of small one at the middle-upper portion of the upstream slope, which are also verified by the result of displacement analysis obtained from integration and filtering of the accelerograms. These experimental results are consistent with the previous seismic damages for earth fill dams and the other results of shaking table dam model tests (Ref.1). The experimental results of pore pressure were reported in Ref.2.

STRAIN POTENTIAL ANALYSIS BASED ON THE CYCLIC TRIAXIAL TEST RESULTS

A method of analysis for predicting earthquake-induced deformations of earth fill dams was firstly proposed by Newmark (Ref.11) and was modified by Seed and his coworkers (e.g. Ref.12). In this section, strain potential is analysed for elements of the shaking table dam model with the FEM programs to verify the applicability of the above-mentioned relations to practical problems. In this numerical procedure, firstly, initial shear stress is analysed using the static nonlinear FEM program with accounting for the construction sequence of fill dams and the effects of seepage. Secondly, the seismic stress history is analysed using the program for evaluating the dynamic response and using the strain-dependent deformation characteristics obtained by cyclic triaxial test. Finally, strain potential and residual pore pressure of elements under a phreatic line are analysed using the program incorporated the quantitatively determining relations. Generally, in the final process, the irregular stress history must be transformed to the equivalent uniform stress series by the procedures such as used in the liquefaction analysis. But this transformation is not used in this investigation because of the sine wave acceleration used. The numerical model of the same scale as the prototype dam is used to apply the nonlinear parameters and the dynamic deformation characteristics obtained by the triaxial test with medium confining stresses. The time scale is magnified 10 times and the sine wave acceleration of 1.5*Hz* frequency and 200 *gals* amplitude is applied for 600 *sec*, which was recorded at the base of the shaking table dam model. Fig.16 shows the contour lines of (a) strain potential ε_p (%) and (b) residual pore pressure ratio u/σ_3, after 50 *sec* for the 200 *gals* model test. This figure shows the large strain potential distribution near the entry and exit points of the phreatic line. This result is consistent with the

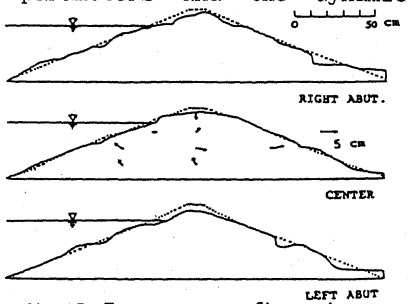

Fig.15. Transverse configurations after dynamic failure test of the shakig table dam model.

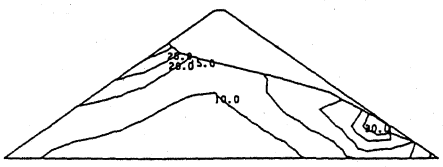

Fig.16(a). Contours of strain potential (after 50 sec).

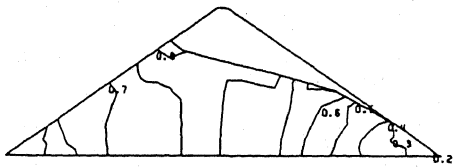

Fig.16(b). Contours of residual pore pressure (after 50 sec).

observational and analytical results for the shaking table model test mentioned above. The results of this strain potential can be used to evaluate the overall deformed configuration of the dam and the stress distribution involving the inertia stresses induced by earthquakes using the procedure such as used in Ref.12. Consequently, the applicability of this procedure is verified to practical problems concerned with earthquake resistant design.

CONCLUSIONS

The following conclusions can be drawn from the present investigation.

(1) The major effect of applying initial shear stress on cyclic triaxial behavior is shown that permanent axial strain increases with number of cycles and the specimen leads to failure. This result is consistent with the previous seismic damages for earth fill dams and the experimental results of shaking table model tests. These facts suggest that earthquake induced permanent deformation of soil under a sloping surface is the most important factor affecting on the dynamic failure of earth fill dams.

(2) It is shown that the dynamic failure criterion can be defined by a specified permanent axial strain, ε_a=10% for the testing soil, which has the basis corresponding to the start point of dynamic failure defined by the point with increment of permanent axial strain reaching constant.

(3) The relations are obtained for quantitative determination of permanent axial strain using void ratio before cyclic loading e_c, effective mean stress level p_m/σ_3, initial shear stress level q_m/p_m, cyclic stress level q_a/p_m and number of cycles N, and the relations for residual pore pressure using e_c, initial shear stress level q_s/q_f and confining stress σ_3.

(4) The FEM program incorporated the above mentioned relations is applied to analyse strain potential for elements of the dam model. As the result of comparing the numerical results with the experimental results for the shaking table dam model, the applicability of this procedure is verified.

REFERENCES

1) Tamura,C., Okamoto,S., Kato,K. and Ohmachi,T. (1975) : Study on mechanism of failure of rockfill dams during earthquakes on results of vibration failure tests of large scale models of the dam, Proc. 4th Japan Earthquake Eng. Symp., pp.703-710 (in Japanese).
2) Kikusawa,M. and Hasegawa,T. (1982) : Dynamic response analysis and model test of an embankment dam, Proc. Int. Symp. on Num. Models in Geomech., Zurich, pp.463-474.
3) Toki,S. and Kitago,S. (1974) : Strength characteristics of dry sand subjected to repeated loading, Soils and Foundations, Vol.14, No.3, pp.25-39.
4) Uchida,K., Sawada,T. and Hasegawa,T. (1980) : Dynamic properties of sand subjected to initial shear stress, Proc. Int. Symp. on Soils under Cyclic and Transient Loading, Swansea, Vol.1, pp.121-133.
5) Marr,W.A.,Jr. and Christian,J.T. (1981) : Permanent displacements due to cyclic wave loading, J. Geotech. Eng. Div., ASCE, Vol.107, No.GT8, pp.1129-1149.
6) Yoshimi,Y. and Oh-oka,H. (1975) : Influence of degree of shear stress reversal on the liquefaction potential of saturated sand, Soils and Foundations, VOL.15, NO.3, pp.27-40.
7) Ohara,S. and Matsuda,H. (1978) : Dynamic shear strength of saturated clay, Proc. JSCE, No.274, pp.69-78 (in Japanese).
8) Houston,W.H. and Herrmann,H.G. (1980) : Undrained cyclic strength of marine soils, J. Geotech. Eng. Div., ASCE, Vol.106, No.GT6, pp.691-712.
9) Ishihara,K. and Nagao,A. (1983) : Analysis of landslides during the 1978 Izu-Oshima-Kinkai earthquake, Soils and Foundations, Vol.23, No.1, pp.19-37.
10) Vaid,Y.P. and Chern,J.C. (1983) : Effect of static shear on resistance to liquefaction, Soils and Foundations, Vol.23, No.1, pp.47-60.
11) Newmark,N.M. (1965) : Effects of Earthquake on Dams and Embankments, Geotechnique, Vol.15, No.2, pp.139-173.
12) Serff,N., Seed,H.B., Makdisi,F.I. and Chang,C.Y. (1976) : Earthquake induced deformations of earth dams, EERC Report, Report No. UCB/EERC-76/4.